Color-Coded Three-Dimensional Micro Particle Tracking Velocimetry and Application to Micro Accelerating Micro-Channel Flow

Wei-Hsin Tien [1], Dana Dabiri [1,*], Jay R. Hove [3]

1: Department of Aeronautics and Astronautics, University of Washington, Seattle, USA
2: Department of Molecular and Cellular Physiology, University of Cincinnati, Cincinnati, USA
* correspondent author: dabiri@u.washington.edu

Abstract In this work the author proposed a microscopic particle tracking system based on the previous work (Tien et al. 2008). A three-pinhole plate, color-coded by color filters of different wavelengths, is utilized to create a triple exposure pattern on the image sensor plane for each particle, and each color channel of the color camera acts as an independent image sensor. This modification increases the particle image density of the original monochrome system by three times, and eliminates the ambiguities caused by overlap of the triangle exposure patterns. A novel lighting method and a color separation algorithm is proposed to overcome the measurement errors due to cross-talk between color filters. A complete post-processing procedure, including a cascade correlation peak-finding algorithm to resolve overlap particles, a calibration-based method to calculate the depth location based on epipolar line search method, and a vision-based particle-tracking algorithm are developed to identify, locate and track the Lagrangian motions of the tracer particles and reconstruct the flow field. This technique is applied to measure a flow over a backward-facing micro-channel flow. The channel/step height is 600 μm / 250 μm. A 10X infinity-corrected microscope, and back-lighted by three individual high power color LEDs aligning to each of the pinhole is used to image the flow. The volume of imaging is 600 × 600 × 600 μm³. The flow field is resolved by particle tracking, and then interpolated using Radial Based Function (RBF) interpolation onto a uniform grid. To validate the flow field resolved from a two-frame tracking method, a steady flow with low particle density and an accelerating flow with high particle density are measured respectively. The Reynolds number in the current work varies from 0.033 to 0.825. 20592 vectors are reconstructed by time-averaged tracking of 156 image pairs from the steady flow case, and roughly 400 vectors per image pair are reconstructed by two-frame tracking from the accelerating flow case. The comparison of the resolved flow fields shows the two-frame tracking method captures the flow field reasonably well.

1. Introduction

Particle Tracking Velocimetry (PTV), like its counterpart, Particle Image Velocimetry (PIV), are whole field measurement techniques for measuring flow velocities in fluid mechanics studies. They are non-intrusive and capable of measuring the whole flow field simultaneously. Both techniques have been improved to meet the requirements of various applications, yet they are still evolving to become a better tool for the researchers to use in many advanced studies. One of the most active areas in recent years is the micro-PIV/PTV, where the techniques are used to imaging the micro-scale flow phenomenon. The first micro-PIV was developed by Santiago et al. (1998) to image a Hale-Shaw flow around a 30 micrometer elliptical cylinder, which was a direct implementation from a macro-scale 2D plane PIV system to a micro-scale system. In the study, epifluorescence microscopy was used to image the tracer particles, and a volumetric illumination from a white light source was used. The velocity fields were measured with spatial resolution down to 6.9 μm × 6.9 μm × 1.5 μm. Since then, most of the 2D micro-PIV/PTV systems use a similar experimental setup, with various data processing techniques to reconstruct the flow field.

The main limitation of the 2D planar PIV/PTV system is that it only measures a slice of the flow with the two co-planar velocity components (2C-2D). Towards this end, we have developed a 3-D technique to overcome this limitation. PTV is more favored than PIV since most of the 3-D techniques are point-based method, meaning that each particle location has to be calculated before resolving the flow field, making

PTV a natural choice for the 3-D techniques. Furthermore, one of the advantages of PTV in micro-scale flow compared to PIV is that higher resolution can be achieved with the same particle density. The cross-correlation based methods like PIV require several particle images in one interrogation window to resolve one reliable velocity vector, while PTV produces a velocity vector from each the particle image. For macro-scale flow, it is not an issue since higher particle concentrations can be achieved and PTV method may encounter difficulties in identifying overlapped particle images accurately. However, due to the high magnification and volumetric illumination used in most of the micro-scale PTV applications, the particle image density is limited in order to achieve acceptable signal to noise ratio. As a result, the resolution of the cross-correlation based methods like PIV is usually lower than PTV methods.

Several 3-D techniques have been developed to overcome this limitation, including stereoscopy (Lindken et al. 2006; Bown et al. 2006), Digital Holographic Microscopy (DHM, Sheng et al. 2006; Satake et al. 2006; Ooms et al. 2009), wavefront sensing (Angarita-Jaimes et al. 2006; Towers et al. 2006; Chen et al. 2009; Cierpka et al. 2010, Cierpka et al. 2011) and defocused techniques (Park and Kihm 2006; Peterson et al. 2008; Luo et al. 2006; Luo and Sun 2011). One of the 3-D techniques uses multiple pinholes to create multiple exposures of the same particle on the image plane to create a certain patterns. The particle location can be calculated by relating the pattern size variation related to the depth location. This concept was first proposed by Willert and Gharib (1992), in which a three-pinhole aperture mask is inserted between the image sensor and the measuring volume. Any particle away from the focal plane forms triple image exposures on the imaging plane, and the distances between each exposure increases as the actual distance of the particle to the focal plane increases. Thus the depth location can be calculated based on the size of the trianglular pattern formed from the three exposures. The technique is successfully applied to the macro-scale flows by Pereira et al. (2000, 2002). Yoon and Kim (2006) first applied the method to a micro-scale backward-facing step flow, and derived a mathematical model to account for effect of the pinhole plate location. A calibration-based method is proposed later by Pereira et al. (2007) as an equivalent optical model of the complicated multi-element microscope system to simplify the calculation. The main advantage of this technique is the potential to have a better balance between computational cost and particle density. Since the depth calculation is purely based on geometric optics, the requirement for computational power is less than those methods based on diffraction patterns or DHM. The particle image density can also be potentially higher than other method, except the DHM technique, since the defocused particle image size is smaller. The major disadvantage is the lower optical efficiency due to the use of small pinholes, which significantly reduced the light allowed to go to the image sensor. In our previous study, Tien et al. (2008) proposed a novel approach using the original three pinhole single camera system, by using a color camera and putting different color filters on each of the pinholes. Since the particle image exposure is color-coded, each color channel acts as an independent image sensor. This modification raised the potential particle image density of the original system by three times, and eliminates the ambiguities caused by overlap of the triangle patterns. With a forward scattering setup, the loss of optical efficiency is largely compensated. Since the potential to resolve flow with high particle density, it is a suitable choice to study unsteady flow phenomenon. In the study the magnification is increased to 2.39 to image a $3.35 \times 2.5 \times 1.5$ mm volume. 25μm diameter polystyrene particle is used to image buoyancy driven flow. In addition, an effective single-lens optical model to represent a multi-element lens system is also proposed that results in better measurements.

In the present work the authors propose a microscopic particle tracking system that has the potential of measuring micro-scale flows by two frame tracking. The system is a miniaturization of previous work (Tien et al., 2008), and modifications are made to resolve the issues encountered in the miniaturization process. To demonstrate the ability of the system, the method is applied to measure an accelerating backward-facing step micro-channel flow. The system principle is described in section 2, including a novel illuminating method, a new color separation algorithm for image pre-processing, and a calibration based method for calculate the depth location based on epipolar line search method. The experimental setup and implementation of the algorithms are described in section 3. The experimental results of the micro-channel flow is shown and discussed in section 4. Finally, the conclusion and the future work are discussed in section 5.

2. Experimental Method

A. System Principle

The color-coded single lens 3D digital particle tracking velocimetry system has two features that make it different from DDPIV systems: color-coded pinholes and white light forward-scattering illumination. Figure 1 shows how the defocused particle image (triplet) on the CCD plane is superimposed from the three pinhole apertures. Since black particles are imaged, these particles will block the white light and form particle shadows on the images emerging from each of the red, green and blue filtered pinhole apertures. This modification provides good contrast between the background and the particle images because the forward-scattering illumination provides more light into the CCD sensor. The color-coded pinholes reduce the ambiguity problem of matching the triplets from a monochrome image and raise the achievable particle image density by a factor of three.

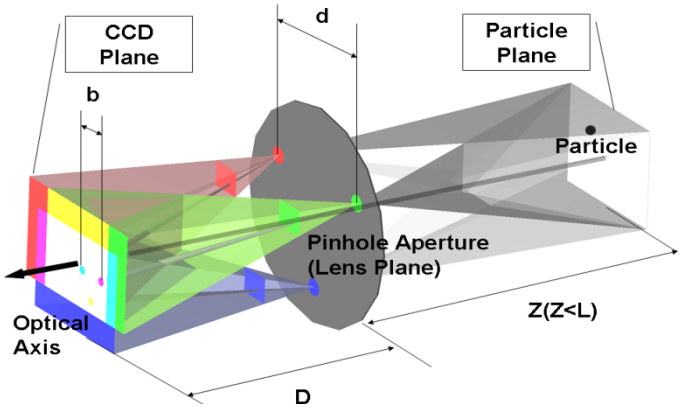

Figure 1. 3D images obtained from a black particle illuminated with backlighting from a white light source through three color filters.

To achieve our purpose of imaging micro-scale fluid flow, the system has to be modified to adapt to the changes of image volume size. The biggest change is to increase the modification of the optical system. In the previous work, a 105mm photographic lens for single lens reflex camera (SLR) is used with a bellow tube to increase the magnification to 2.69. In the current system, a microscope system is used and the minimum magnification is 10. The huge difference in magnification increases the aberration of the optics, especially the chromatic aberration. The chromatic aberration causes different wavelengths of light to have different focal lengths, and it affects the imaging system in several ways. Thus modifications are made to adapt the color-coded single lens defocusing system to be suitable for microscopic applications. We therefore call this the 3D-μPTV system.

B. Illumination Method

The color aberration shifts the peak locations of the particle images. The image profile of a particle under illumination produced by a diffraction limited imaging system can be approximated by a Gaussian distribution (Adrian and Westerweel, 2011), and the peak location is used to calculate the particle location. A typical spectral response of the pinhole color filters is not a narrow band-pass filter because it is desirable to collect the light as much as possible for an incoherent light source. Therefore the spectral response of white light passing through a filter is still an integral contains all wavelengths of light, just with a weighting distribution that suppresses wavelengths other than the dominant wavelength of the filter.

For a perfect optical system with no color aberration, the peak location is the same for all wavelengths of light, so the peak calculated from the particle image profile based on the Gaussian shape assumption is accurate. However, with color aberration, the peak location for different wavelengths deviates from each other, as shown in Figure 2(a). Thus the calculated peak location shifts from the true peak location and contribute to the measurement error of the system (Figure 2(b)). The amount of shift is a function of the particle physical location, and therefore cannot be corrected without knowing the particle location first.

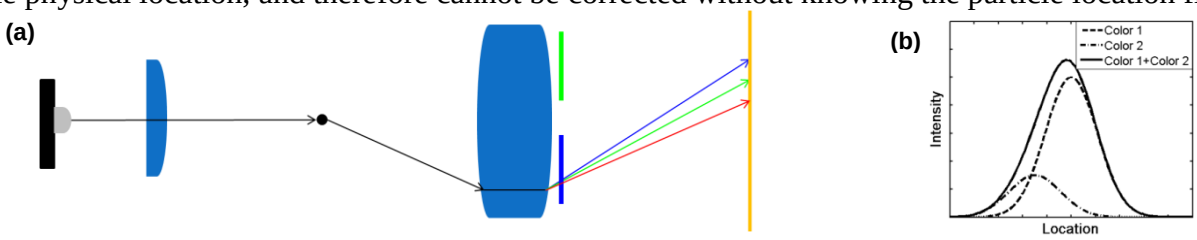

Figure 2. Particle image peak shifts due to color aberration: (a) color aberration due to white light illumination, (b) The skewed Gaussian distribution due to the peak shifts.

To resolve this issue without using narrow-band filters and reducing the light intensity, a new configuration of lighting is used for the 3D-μPTV system. As show in Figure 3, each pinhole is now aligned with a individual light source with corresponding color to match the spectral response of the color filter on each pinhole. Because the light is from an inclined angle aligned to the corresponding pinhole, the scattering angle of the light to the other two pinholes are significantly redirected away from their former optimized scattering angle (≈ 0º). Therefore, only the wavelength of light coming from the matched light source results in the particle image exposure for the corresponding pinhole, and the peak shift due to color aberration can be minimized.

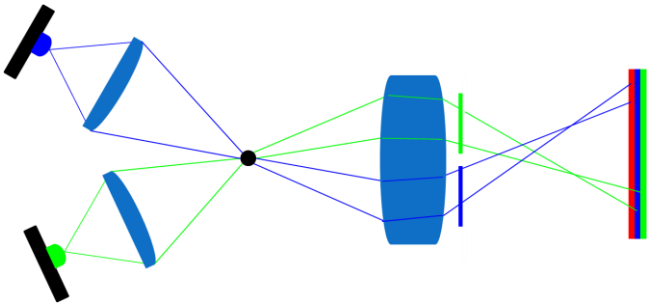

Figure 3. Novel illumination configuration.

C. Color Separation

A method for separating the three colors is necessary to identify the color-coded triplet images taken by this system. In theory, this can be easily done if the spectra of each of the red, green, and blue color filters perfectly match the spectra of each of the red, green, and blue sensors, respectively, since light emerging from each of the color filtered pinholes would expose only on their respective sensor. In reality, the spectra of the color filters and the image sensors do not match, thereby causing multiple pinhole exposures on each of the image sensors. Due to the signal crosstalk between the color channels of the image sensor, multiple exposures still happens even a single wavelength light passing through each pinhole. As shown in Figure 4(a), the typical spectral response of the color filters used in a CCD camera shows overlap region between color channels. Wavelengths of light falling in these regions creates signal bleed-through to both color channels, thus causing multiple exposure images at the same location through each pinhole with the corresponding single color light source, as shown in Figure 4(b). Thus a new algorithm to separate the color is developed to resolve this issue.

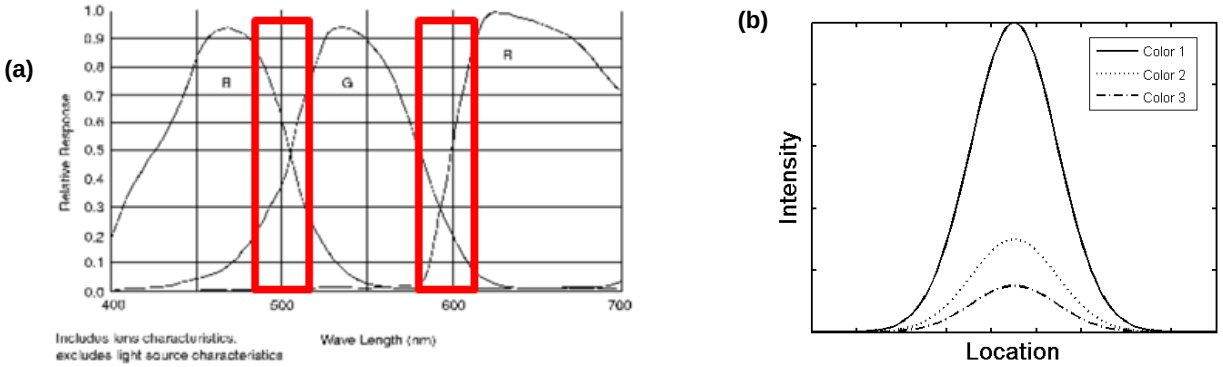

Figure 4. Multiple exposures caused by signal bleed-through: (a) spectral response of a CCD sensor. The black rectangles show the overlap regions of the spectral response. (b) multiple exposures from the same wavelength of light to different color channels. Color 1 is the response from the dominant wavelength.

Eliminating the crosstalk between color channels is equivalent to decorrelating the image data from

the color channels. Using principal component transformation (PCT, Richards and Jia (1999)), the image data based on the correlated R, G and B primaries can be decorrelated to form a new image based on three independent new primaries. For each pixel of the image, the color can be expressed as

$$\mathbf{C}_{ij} = \begin{bmatrix} R_{ij} \\ G_{ij} \\ B_{ij} \end{bmatrix} \quad (1)$$

,

where *R, G, B* are values in term of the original primaries. It can also be expressed as

$$\mathbf{C}_{ij}' = \begin{bmatrix} R_{ij}' \\ G_{ij}' \\ B_{ij}' \end{bmatrix} \quad (2)$$

,

where R'_{ij}, G'_{ij} and B'_{ij} are values in term of the new uncorrelated primaries. Thus C'_{ij} is related to C_{ij} by a transformation matrix T: $\mathbf{C}_{ij}' = \mathbf{T}\mathbf{C}_{ij}$.

The advantage of this method is that it is adaptive, so no parameter is required throughout the process, and the results are more robust to the variations of lighting. Figure 5 shows the result of color separation using the proposed algorithm. In the circled region, two green particles can be seen from both the green and blue channels before color separation, but after the color separation, only the new green channel keeps the two particle images.

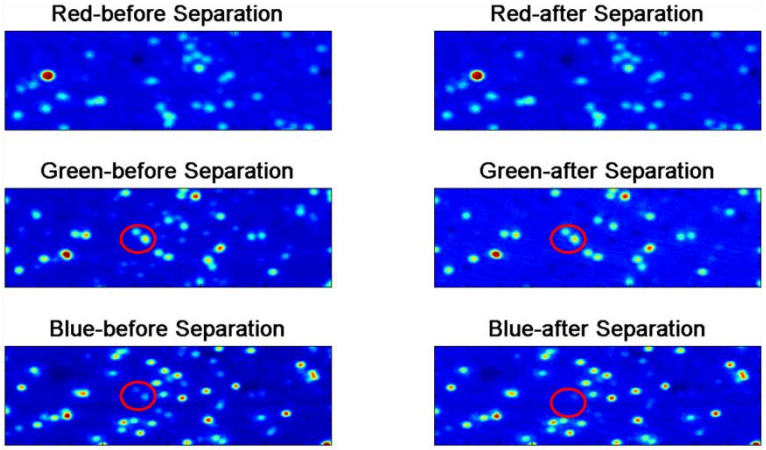

Figure 5. Results of color separation algorithm.

D. Particle Identification

The high magnification of the microscope optics with the pinhole configuration also changed the particle image size significantly. A typical particle image size from a 3D-μPTV image is around 25 pixels, since we are imaging a depth that extends beyond the focal plane; this is much larger than the 2-4 pixel diameter usually encountered in traditional 2-D PIV/PTV applications. As a result, the chance of a particle image overlap with another one increases drastically. Severe particle overlap would cause location errors of the peak and are critical to velocity measurement errors. To identify the particle image peak location more accurately, a particle identification algorithm, modified CCM Algorithm (Lei et al.) is used to improve the ability to identify overlap particle images.

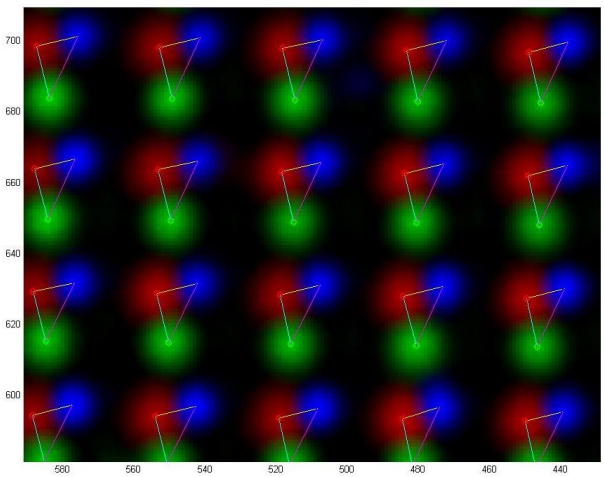

triplet exposures due to chromatic aberration.

E. Particle Location Calculation

For the 3D-μPTV system, the chromatic aberration also causes equilateral triangle patterns to be seriously skew (Figure 6). Thus the characteristic equations derived in the DDPIV systems (Tien et al. (2008), Kajitani and Dabiri (2005), Grothe and Dabiri (2008)) do not describe this system. This affects both the

triplet finding and particle location calculations, since in the previous work both processes rely on the DDPIV characteristic equations. Thus a calibration-based method is developed to first match the triplet particle images of a particle from each color channel, and then the particle location in physical space is calculated based on the calibration results.

Our 3-D μPTV system is developed as a system with three pinhole camera views; the epipolar line search method proposed by Maas et al. (1993) can be applied to the 3-D μPTV system to find the triplet match. The epipolar line has to be generated from any image point in the image plane from a specific image point in another image plane. This can be done by finding the line of projection of the point of interest and then project it to the plane where the epipolar line is to be found in. For instance, in **Error! Reference source not found.**, the line of projection O_LP_1 can be calculated from x_{L1} in the left image plane and the epipolar line $e_{L\text{-}R}$ can be found by projecting P_1 and P_3 to x_{r1} and x_{r3} in the right image plane. The calculation of line of projections requires a full optical model of the system. The optical system is usually approximated by a pinhole camera model, and the camera parameters are found through a calibration procedure (Maas, et al., 1993). However, due to the high magnification and larger depth of field with the pinhole, the accuracy of the simple pinhole model is not enough and the ability to correct image distortion at different depths is important. Thus, we model the optical system of the 3-D μPTV by developing a calibration-based procedure that is similar to Maas' epipolar line search method.

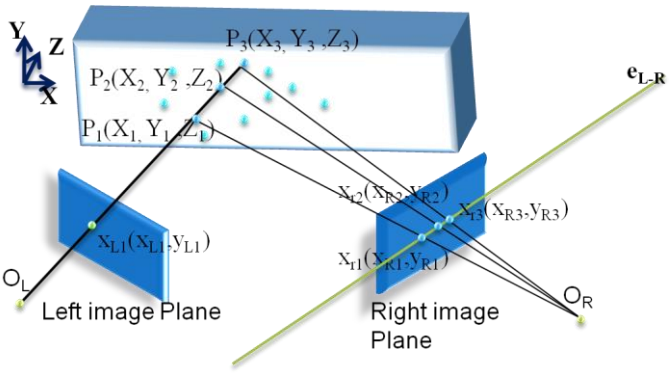

Figure 7. Epipolar geometry.

The calibration procedure is explained by Figure 8. A target plate with an array of dots is set to move to different positions. At each position, the calibration images are taken with the left and right cameras. Each calibration image is processed through the peak-finding algorithm introduced in section D to find the projected peak locations. The projected peak locations from each image plane and the true physical positions of the calibration dots can be related by mapping functions

$$x_R = f_{x,L\Rightarrow R}(x_L, y_L, Z) \qquad y_R = f_{y,L\Rightarrow R}(x_L, y_L, Z)$$
$$x_L = f_{x,R\Rightarrow L}(x_R, y_R, Z) \qquad y_L = f_{y,R\Rightarrow L}(x_R, y_R, Z) \quad (3)$$

$$X = F_{X,L\Rightarrow XYZ}(x_L, y_L, Z) \qquad Y = F_{Y,L\Rightarrow XYZ}(x_L, y_L, Z)$$
$$X = F_{X,R\Rightarrow XYZ}(x_R, y_R, Z) \qquad Y = F_{Y,R\Rightarrow XYZ}(x_R, y_R, Z) \quad (4)$$

where (X, Y, Z) are the physical coordinates of the dot, (x_L, y_L) are the image coordinates of the projected peak location in the left image plane and (x_R, y_R) are the image coordinates of the projected peak location in the right image plane. The functions are approximated with radial base functions (RBF) written in a MATLAB routine by Chirokov (2012), and same procedure is performed for each pinhole pair (red to green, green to blue and blue to red). Once these functions are built, epipolar line can be created for any point in the image plane with eq. (3). For triplet matching procedure, eq. (4) is used for calculating the particle locations in experiments.

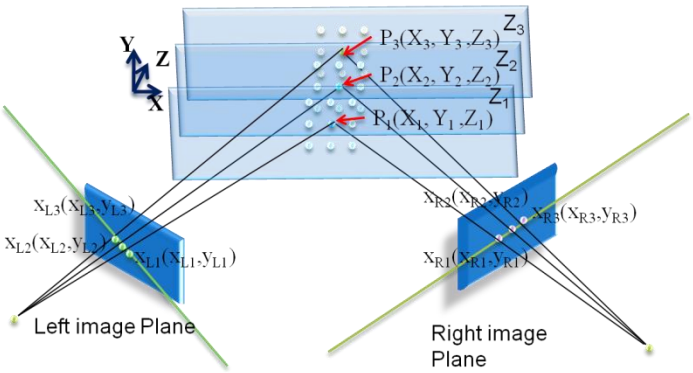

Figure 8. Calibration Procedure.

In the actual experiment, once the image triplets of a particle are matched by the epipolar line search method, the next step is to calculate the physical coordinates of the particle location (X_p, Y_p, Z_p) based on the peak image coordinates(x_r, y_r),(x_g,y_g) and $(x_b.y_b)$ of red, green and blue pinhole respectively. The Z coordinate is first to be found from eq. (3). It is calculated iteratively by a minimum search routine based on a derivative-free method. Once the Z coordinate is found, eq. (4) is used to calculate the X and Y

coordinates of the particle location. Only two of the peak locations are necessary, but all three pinhole pairs (red to green, green to blue and blue to red) are used to get the coordinates, and the average values are used to improve the accuracy.

After particle locations from two time frames are found, the last processing stage of the 3-D µPTV system is to find the velocity field. In the current work the particle tracking algorithm, based on the original Scott and Longuet-Higgins (1991) method, is an adaptation of our previous work (Lei et al., 2012), but expand it from 2-D to 3-D. The implementation of the method is hybridized with PIV results, and an iterative scheme with outlier detection method by Duncan et al. (2010) is used to increase the robustness and accuracy of the method. The guiding 3-D PIV field is built using a 3-D cross-correlation method developed by Pereira *et al*. (2000).

F. Experimental Setup

The 3D-µPTV system is developed and tested based on the principles introduced in the previous section. Figure 9 shows a schematic of the current 3D-µPTV system setup. To demonstrate the capability of the system, a micro-scale backward-facing step flow is set up and the flow field is resolved by the 3D-µPTV system. The experimental apparatus consists of four major components: the infinity-corrected inverted microscope system, the micro-channel flow system, the calibration system and the data processing software.

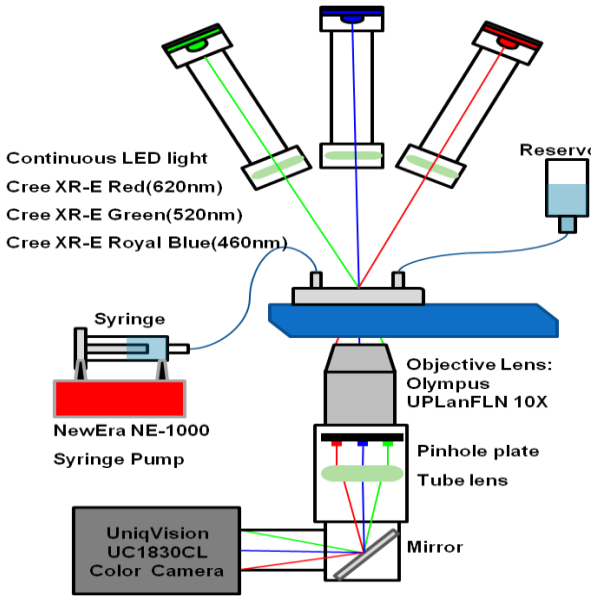

Figure 9. Schematic of 3-D µPTV experimental setup.

Since the 3D-µPTV system is designed to measure fluid flow in micro-scales, the requirement for magnification (usually >10) makes the microscope system a critical component of the system. In order to have more flexibility to test different optical configurations, a customized inverted microscope system is designed and assembled. As shown in Figure 9, the lights are set on top and the objective lens is put underneath the flow model. The main reason to choose the inverted configuration is for the ease of testing different lighting configurations, and it also provides an easy access for aligning the calibration target and micro-channel model, since it has a longer working distance to the light source In the current setup, both the objective lens (Olympus UPLanFLN 10X) and the tube lens (U-TLU) are made by Olympus to insure the optical performances are matched. Due to the additional length of the adapter ring for the camera mounting, the actual magnification measured from the image of a target plate is 10.965 instead of 10.

The 3-pinhole plate is placed in the objective lens right after the lens elements. The diameter of each pinhole is d=1.5 mm, and the distance R (from the pattern center to each pinhole center) is 3 mm, results in a pinhole separation distance of 5.196mm. The current configuration results in a measurable image volume of 600 × 600 × 600 µm^3.

High power LEDs (light-emitting diode) are used as the light source of the system. Compared with other incoherent light sources, the main advantage of LEDs is that they have the narrow spectral widths. The spectral width (full width at half maximum, FWHW) of a typical quasi-monochromatic LED varies from 20~40 nanometers, which is ideal to match the spectral response of those pinhole color filters. In the current system, three Cree XR-E series LEDs with Red (620 nm), Green (520nm) and Royal Blue (460 nm) are used to provide a continuous light source. Critical illumination configuration is used where each LED is aligned with a lens doublet to focus the light to the object plane. A 1024 pixel × 1024 pixel resolution color CCD camera (uniqvision UC-1830CL) of a frame rate of 30 frame per second is used to capture the images. The typical exposure time is set to 4.167 ms (1/240 s). The data rate is 30 Hz. Images are captured and recorded by software (Video Savant® 4, IO Industries Inc.) through a frame grabber

board (Road Runner R3 CL, Bitflow Inc.) in a PC.

A calibration apparatus is constructed to perform the calibration procedure presented in section E. As shown in Figure 10(a), the calibration target is a 50 mm × 25 mm × 1.52 mm glass plate with grid arrays of blue chrome dots. The size of each dot is 3 μm with a grid spacing of 20 μm (Figure 10 (b)). The target plate is connected to a 6-axis translation stage (APT 600, Thorlabs). The stage is used to align the calibration target with the optical axis of microscope system to provide the accurate position in Z-axis of the target for each calibration plane. A glass slide of the same size to the bottom glass plate used for the micro-channel model is put in between the objective lens and the calibration target. By putting water in between the glass slide and the target plate, the refraction effect of water the glass material is matched this way during calibration. A total of 14 planes data are taken, with 25 μm spacing in the Z-axis. The focal plane is set to the mid-plane of the 14 calibration planes and centered around the step so that the measurable volume covers the whole microchannel. Figure 10(c) shows a typical calibration image taken during the calibration test.

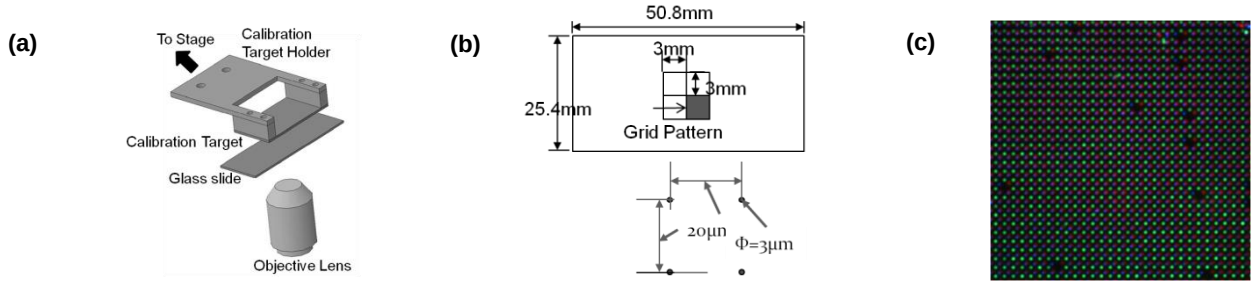

Figure 10. System Calibration: (a) Experimental Setup (b) Target plate pattern (c) Example of a calibration image.

A backward-facing step flow micro-channel is constructed to test the performance of the 3D-μPTV system (Figure 11). A piece of 22 mm × 6 mm × 0.2 mm thin glass plate cut from a cover glass is glued to a 75 mm × 25 mm glass slide to form the step of the flow channel. The top wall is a transparent plexiglas plate cut to the same size as the bottom glass slide and glued together by double-sided PMMA (Poly (methyl methacrylate)) tape and a thin layer of epoxy glue. The tape and glue are also served as the side walls of the micro-channel. Both the top and bottom walls are transparent to ensure clear optical access for lighting the volume of interest. The resulting channel dimension is 22 mm × 6 mm × 0.35 mm before the step and 15 mm × 6mm × 0.6 mm after the step. The laminar flow is driven by a syringe pump (NewEra NE-1000), and deionized (DI) water is used as the working fluid. 2 μm polystyrene particles (Polybead® Microspheres, Polysciences Inc.) are used as the tracer particles.

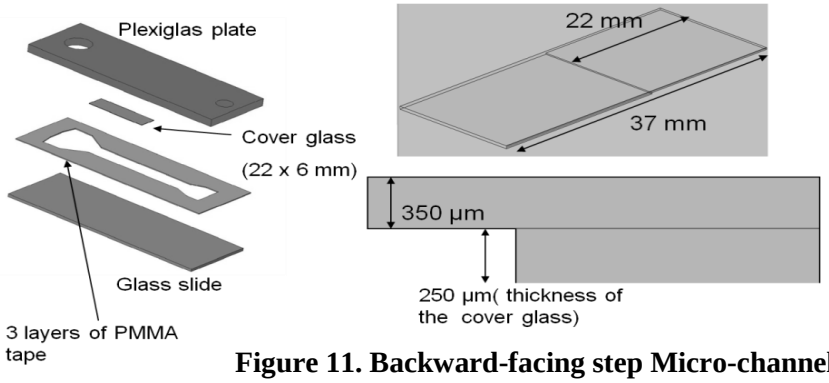

Figure 11. Backward-facing step Micro-channel.

The data processing software is coded in MATLAB (Mathworks, Natick, MA). Video captured by the data recording software is saved in individual frames in 24-bit color image format, and the final data output is the particle locations in physical space.

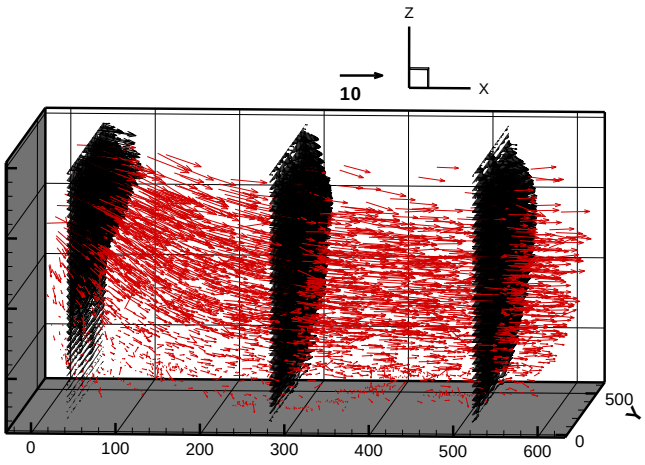

Figure 12. Resolved Backward-facing step flow field: Steady Flow.

3. Experimental Results

The true test of the performance of 3-D μPTV system is of course to resolve a real flow case. The backward facing step flow micro-channel is used for this purpose. The main advantage of the 3-D μPTV system based on the color-coded pinhole system is the possibility to increase the particle density. Most of the current 3-D techniques are limited to low particle density; as a result, they have to rely on time-averaging to get enough data to resolve the whole flow field and the consequence is that the flow field has to be steady. Thus it is important to test if the proposed new technique can be used to break this limitation.

A. Steady Flow

The first experiment is to verify the system performance with a steady flow. Using the set up presented in section F, the flow is maintained at 40 μl/min which corresponds to a Reynolds number Re =0.22. The field of view is located right after the backward-facing step with an imaged volume of 600 ×600×600 μm^3. 156 image pairs are processed and the results are overlapped to one field, as shown in Figure 12. (red vectors). A total of 20592 vectors are identified, indicating an average of 132 vectors per image pair. Using RBF interpolation, the PTV result is interpolated to a uniform grid spacing on the size of 10 μm × 10 μm × 10 μm, as shown in fig. 12 (Black vectors, only showing the representative planes). The flow field result clearly shows the flow structure after the step with high spatial resolution.

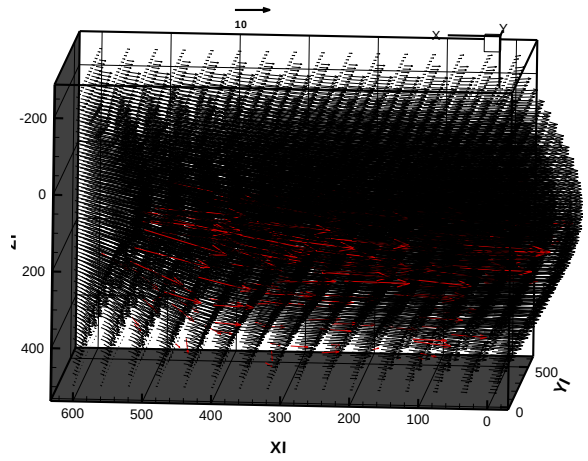

Figure 13. Resolved Backward-facing step flow field: Decelerating Flow at the start.

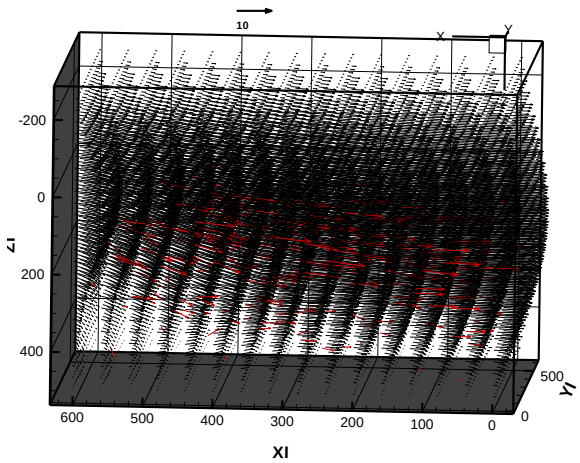

Figure 14. Resolved Backward-facing step flow field: Decelerating Flow at the end.

B. Unsteady Flow

The second experiment is to explore the possibility to use only one image pair to resolve the flow field with reasonable spatial resolution for a unsteady flow. The unsteady backward-facing step flow is created by decelerating the constant flow rate at 150 μl/min by 12 step decrements at 12 μl/min, resulting in the Reynolds number changing from 0.825 to 0.033.The imaged volume is 600 ×600×600 μm^3, as in the steady flow case. The syringe and the tubing provide a damping effect, so the flow is decelerating smoothly without step change. Figure 14 shows the vector field using particle tracking results from the starting frame pair (Q = 150 μl/min). A total of 392 vectors are identified in an image pair, shown in the red vectors, and the corresponding interpolated vector field (black vectors) on a uniform grid of size of 40 μm

× 40 μm × 30 μm. The spatial resolution is lower than the time-averaged case, but the flow features are still captured extremely well. Figure 14 shows the vector field of particle tracking results from the ending frame pair (Q = 6 μl/min). A total of 444 vectors are identified in a image pair, shown in the red vectors, and the corresponding interpolated vector field (black vectors) on a uniform grid of size of 40 μm × 40 μm × 30 μm. These results indicate that the unsteady flow can be resolved with our 3-D μPTV technique.

G. Conclusion

A novel three-dimensional micro particle tracking velocimetry technique is developed using a single color camera. By modifying the illumination method and adopting several new processing algorithms, this 3-D micro particle tracking velocimetry is able to measure a flow inside a 600μm × 600μm × 600μm volume with high spatial and temporal resolution. A micro-scale backward-facing step flow is resolved in both steady and decelerating flow conditions, ranging from Reynolds number 0.825 to 0.033. These results show that the proposed technique is able to capture micro-scale flow with high spatial resolution in a cubic volume, which provides the technique to capture larger three-dimensional flow structure than other 3-D techniques. This technique also achieves a high enough particle image density that can provides necessary temporal resolution to resolve unsteady flow.

H. Acknowledgments

The authors gratefully acknowledge the support of the National Institutes of Health (R01 RR023190-04) and the Murdock Trust Foundation.

References

Adrian RJ & Westerweel J (2011) Particle Image Velocimetry. Cambridge University Press, Cambridge, New York.

Angarita-Jaimes N, McGhee E, Chennaoui M, Campbell HI, Zhang S, Towers CE, Greenaway AH & Towers DP (2006) Wavefront sensing for single view three-component three-dimensional flow velocimetry. Experiments in Fluids 41(6): 881-891.

Bown MR, MacInnes JM, Allen RWK & Zimmerman, WBJ (2006) Three-dimensional, three-component velocity measurements using stereoscopic micro-PIV and PTV. Measurement Science & Technology 17(8) 2175-2185.

Chen S, Angarita-Jaimes N, Angarita-Jaimes D, Pelc B, Greenaway AH, Towers CE, Lin D & Towers DP (2009) Wavefront sensing for three-component three-dimensional flow velocimetry in microfluidics. Experiments in Fluids 47(4-5): 849-863.

Chirokov, A (2012) Scattered Data Interpolation and Approximation using Radial Base Functions. URL: http://www.mathworks.com/matlabcentral/fileexchange/10056-scattered-data-interpolation-and-approximation-using-radial-base-functions.

Cierpka C, Rossi M, Segura R & Kaehler CJ (2011) On the calibration of astigmatism particle tracking velocimetry for microflows. Measurement Science & Technology 22(1): 015401.

Cierpka C, Segura R, Hain R & Kaehler CJ (2010) A simple single camera 3C3D velocity measurement technique without errors due to depth of correlation and spatial averaging for microfluidics. Measurement Science & Technology 21(4): 045401.

Duncan J, Dabiri D, Hove J & Gharib M (2010) Universal outlier detection for particle image velocimetry (PIV) and particle tracking velocimetry (PTV) data. Measurement Science & Technology 21(5): 057002.

Grothe R, Rixon G, Dabiri D (2008) An Improved Three-Dimensional Characterization of Defocusing Digital Particle Image Velocimetry (DDPIV) Based on a New Imaging Volume Definition, Measurement Science and Technology 19: 065402

Kajitani L & Dabiri D (2005) A full three-dimensional characterization of defocusing digital particle image velocimetry. Measurement Science & Technology 16(3): 790-804.

Lei Y, Tien W, Duncan J, Paul M, Dabiri D, Rösgen T, Hove J, A vision-based hybrid particle tracking velocimetry (PTV) technique using a modified cascade-correlation peak-finding method. Experiments in Fluids (accepted for publication, 2012)

Lindken R, Westerweel J & Wieneke B (2006) Stereoscopic micro particle image velocimetry. Experiments in Fluids 41(2):161-171.

Luo R & Sun Y (2011) Pattern matching for three-dimensional tracking of sub-micron fluorescent particles. Measurement Science & Technology 22(4): 045402.

Luo R, Yang XY, Peng XF & Sun YF (2006) Three-dimensional tracking of fluorescent particles applied to micro-fluidic measurements. Journal of Micromechanics and Microengineering 16(8): 1689-1699.

Maas HG, Gruen A & Papantoniou D (1993) Particle Tracking Velocimetry in 3-Dimensional Flows .1. Photogrammetric Determination of Particle Coordinates. Experiments in Fluids 15(2): 133-146.

Ooms TA, Lindken R & Westerweel J (2009) Digital holographic microscopy applied to measurement of a flow in a T-shaped micromixer. Experiments in Fluids 47(6): 941-955.

Park JS & Kihm KD (2006) Three-dimensional micro-PTV using deconvolution microscopy. Experiments in Fluids 40(3): 491-499.

Pereira F, Gharib M, Dabiri D & Modarress D (2000) Defocusing digital particle image velocimetry: a 3-component 3-dimensional DPIV measurement technique. Application to bubbly flows. Experiments in Fluids 29: S78-S84.

Pereira F & Gharib M (2002) Defocusing digital particle image velocimetry and the three-dimensional characterization of two-phase flows. Measurement Science & Technology 13(5): 683-694.

Pereira F, Lu J, Castano-Graff E & Gharib M (2007) Microscale 3D flow mapping with mu DDPIV. Experiments in Fluids 42(4): 589-599.

Peterson SD, Chuang H & Wereley ST (2008) Three-dimensional particle tracking using micro-particle image velocimetry hardware. Measurement Science & Technology 19(11): 115406.

Pratt, WK (1991) Digital image processing. Wiley, New York.

Richards JA & Jia X (1999) Remote sensing digital image analysis : an introduction. Springer, Berlin, New York.

Santiago J, Wereley S, Meinhart C, Beebe D & Adrian R (1998) A particle image velocimetry system for microfluidics. Experiments in Fluids 25(4): 316-319.

Satake S, Kunugi T, Sato K, Ito T, Kanamori H & Taniguchi J (2006) Measurements of 3D flow in a micro-pipe via micro digital holographic particle tracking velocimetry. Measurement Science & Technology 17(7) 1647-1651.

Scott, GL & Longuet-higgins, HC (1991) An Algorithm for Associating the Features of 2 Images. Proceedings of the Royal Society of London Series B-Biological Sciences 244 (1309): 21-26.

Sheng J, Malkiel E & Katz J (2006) Digital holographic microscope for measuring three-dimensional particle distributions and motions. Applied Optics 45(16): 3893-3901.

Tien, W, Kartes, P, Yamasaki, T & Dabiri, D (2008) A color-coded backlighted defocusing digital particle image velocimetry system. Experiments in Fluids 44(6): 1015-1026.

Towers CE, Towers DP, Campbell HI, Zhang SJ & Greenaway AH (2006) Three-dimensional particle imaging by wavefront sensing. Optics Letters 31(9): 1220-1222.

Willert CE and Gharib M (1992) Three-dimensional particle imaging with a single camera. Experiments in Fluids 12: 353-358.

Yoon SY & Kim KC (2006) 3D particle position and 3D velocity field measurement in a microvolume via the defocusing concept. Measurement Science & Technology 17(11): 2897-2905.